Electrical System for Autonomous Underwater Vehicle and Autonomous Surface Vehicle

Submitted by

Vanessa Cassandra

Department of Electrical and Computer Engineering

In partial fulfillment of the requirements for the

Degree of Bachelor of Engineering

National University of Singapore

Abstract

Team Bumblebee has been developing Bumblebee Autonomous Underwater Vehicle (AUV) version 3.0 since August 2014 and it finally made its debut during Singapore Autonomous Underwater Vehicle Challenge in March 2016. From the initial stage of conception until the deployment of the vehicle, there are problems that were not foreseen and only arose during operation. Improvements need to be made to make the system more robust and reliable.

Team Bumblebee has also started the development of an Autonomous Surface Vehicle (ASV) and it will be deployed during Maritime RobotX Challenge in December 2016.

This paper discusses the improvements that can be made for Bumblebee AUV version 3.0 to ensure a stable system and also about the electrical architecture of the ASV.

Acknowledgement

First and foremost, I would like to express my gratitude to God, who gave me an opportunity to work on a project that I care about, and my strength in times of weary.

I would also like to express my gratitude to my supervising professor, Professor Mandar Anil Chitre, who gave me the opportunity to work under his supervision. I really appreciate the freedom given for me on how to carry out my project and his guidance throughout the project.

I would also like to thank the members of Team Bumblebee for giving me the platform for the project. They give me moral support as comrades with the same cause.

There are many people who contributed to my life and this project that I am not able to mention one by one, but their contribution will not be forgotten.

Table of Contents

List of Figures

List of Tables

List of Symbols and Abbreviations

AGM	Absorbed Glass Mat
AHRS	Attitude Reference Heading System
ASV	Autonomous Surface Vehicle
AUV	Autonomous Underwater Vehicle
CAN	Controller Area Network
DC	Direct Current
DoD	Depth of Discharge
GEDC	Gyro Enhanced Attitude & Heading System
GigE	Gigabit Ethernet
IMU	Inertial Measurement Unit
Li-po	Lithium-polymer
LED	Light Emitting Diode
MCU	Microcontroller Unit
MOSFT	Metal-oxide Field Effect Transistor
N-MOSFET	N-channel Metal-oxide Field Effect Transistor
P-MOSFET	P-channel Metal-oxide Field Effect Transistor
PCB	Printed Circuit Board
POE	Power over Ethernet
PWM	Pulse Width Modulation
RJ45	Registered Jack 45
SBC	Single Board Computer
TTL	Transistor-Transistor Logic
UART	Universal Asynchronous Receiver/Transmitter
USB	Universal Serial Bus

A	Ampere
Ah	Ampere hour
kg	kilogram
kgf	kilogram-force
lbs	pound
m	meter
s	second
V	Volt
W	Watts
Ω	Ohm

1 Introduction

1.1. Background of the project

Bumblebee Autonomous Underwater Vehicle (BBAUV) is a student-led group formed in Summer 2012 by five students in the Mechanical Engineering department. The team develops an Autonomous Underwater Vehicle (AUV) to compete in two international competitions every year: Singapore Autonomous Underwater Vehicle Challenge (SAUVC) and RoboSub competition in San Diego, USA.

Over the years, the team has developed three vehicles, which are Bumblebee 1.0, Bumblebee 2.0, and the latest, Bumblebee 3.0.

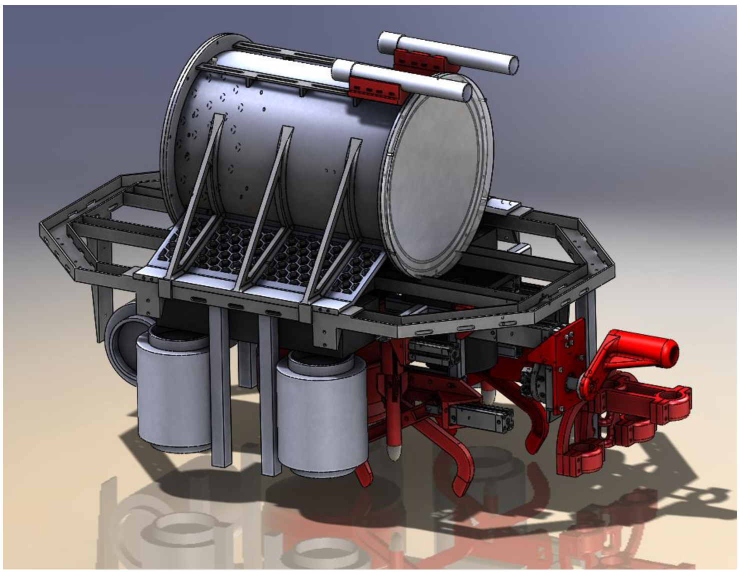

Figure 1. Bumblebee AUV 1.0

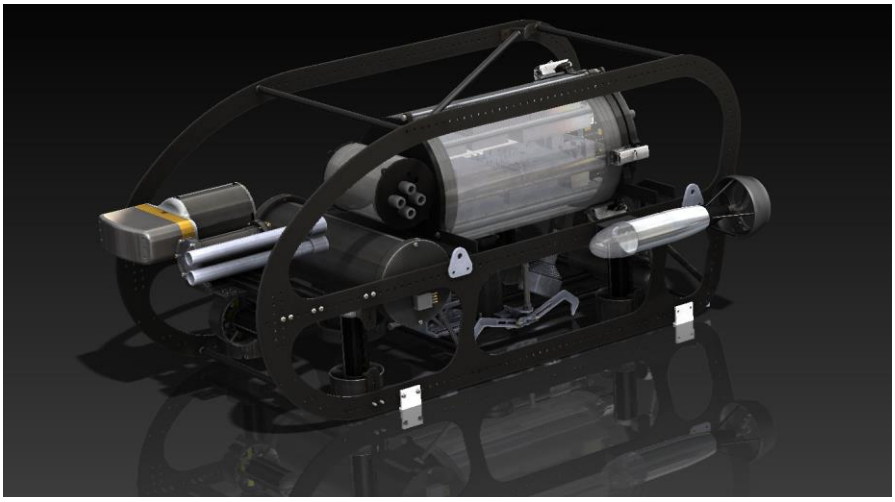

Figure 2. Bumblebee AUV 2.0

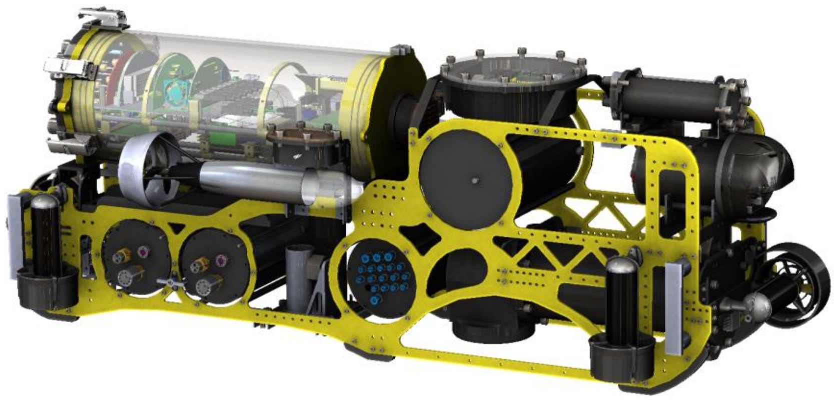

Figure 3. Bumblebee AUV 3.0

As part of the team vision, “To engineer the autonomous system of the future”, Team Bumblebee decided to venture to other unmanned system domain, the Autonomous Surface Vessel (ASV). The team is going to develop an ASV on a Wave Adaptive Modular Vessel (WAM-V) platform and participate in Maritime RobotX Challenge that is held once in two years.

Figure 4. WAM-V platform for an ASV (www.wam-v.com)

The next Maritime RobotX Challenge will be held in Hawaii in December 2016. The teams participating are required to produce the propulsion, control, and sensor systems necessary to complete the competition tasks. The competition consists of tasks such as demonstrating navigation and control, acoustic signal localisation, identification of symbols and colours, and obstacles detection and avoidance.

1.2. Aim of the project

This project's objective is to improve the electrical system of the Bumblebee 3.0, especially on the electrical backplane, and also to choose appropriate electronics components for the ASV and to design a custom electronics board to interface the components with the main processing unit, the Single Board Computer (SBC).

1.3. Scope of the project

1. To identify the existing electrical problems in Bumblebee AUV 3.0
2. To explore and provide solutions to the problems

3. To choose appropriate electronics components, namely the thrusters, batteries, and sensors of the ASV
4. To design an electronics board to interface these components with the main computer.

2 Autonomous Underwater Vehicle (AUV)

The current electrical system of Bumblebee AUV 3.0 is as described in the block diagrams below:

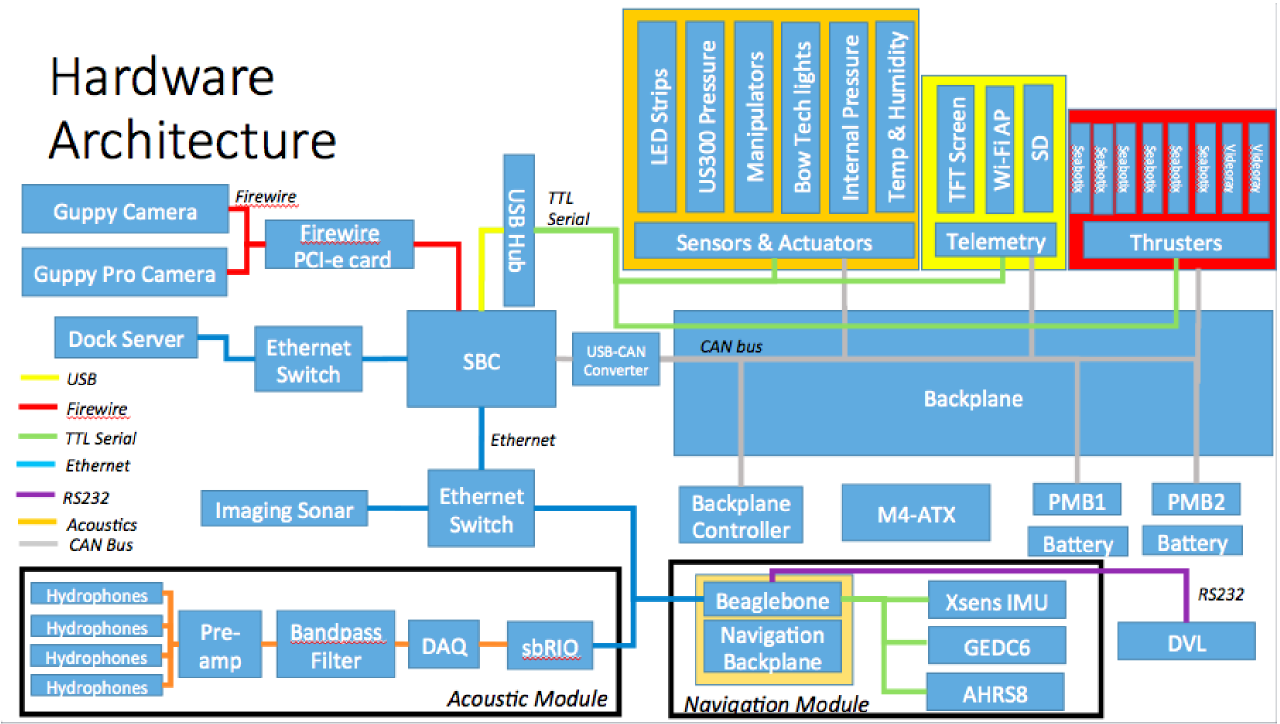

Figure 5. Bumblebee AUV 3.0 Hardware Architecture

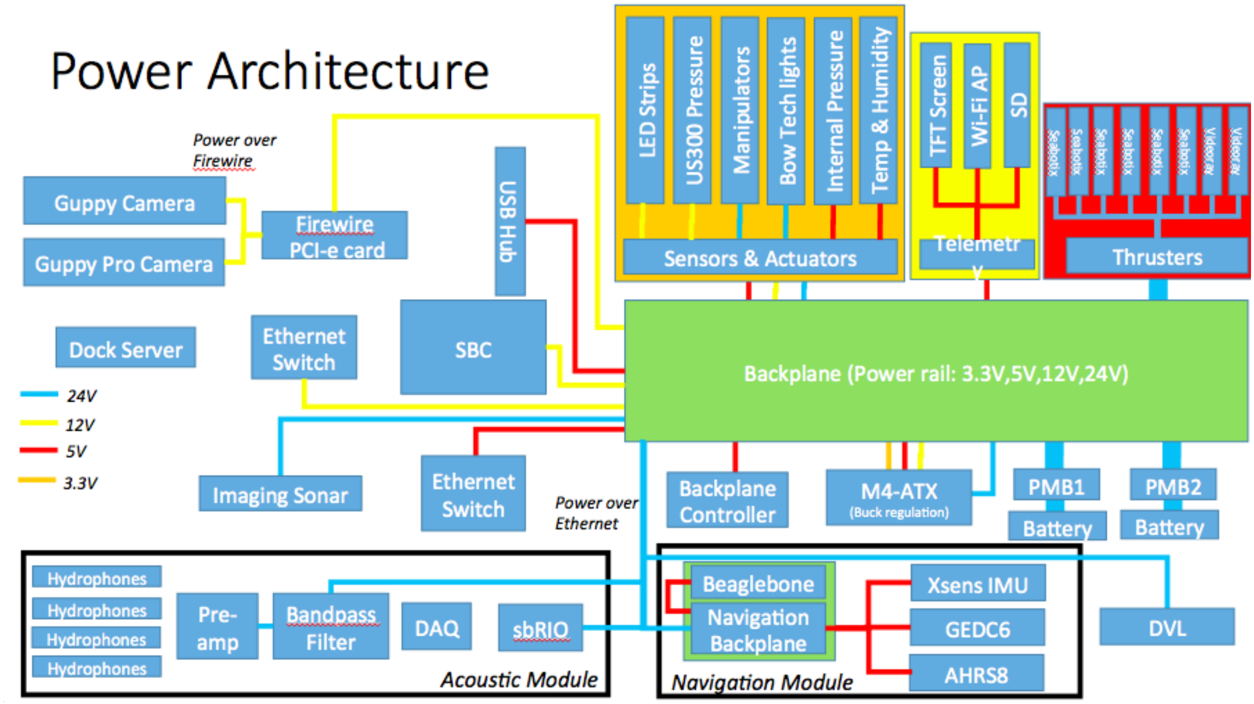

Figure 6. Bumblebee AUV 3.0 Power Architecture

Bumblebee 3.0 runs on two 24V Lithium-polymer (Li-po) batteries each with 7800mAh capacity. The power is directed to the electrical backplane, and then to the M4-ATX, the voltage regulator, and different power rails are then routed back to the electrical backplane to be distributed to other peripherals.

In terms of data connectivity, the Single Board Computer (SBC) is the central processing unit. The SBC is connected to National Instruments' sbRIO in the acoustics sub-system, BeagleBone Black in the navigation sub-system, and the imaging sonar through Ethernet connection. It interfaces with the Guppy and Guppy Pro camera through FireWire protocol. The SBC is also connected to other electrical components using Controller Area Network (CAN) protocol. Additional Serial link from the SBC is used to program the MCU on board.

3 AUV Backplane

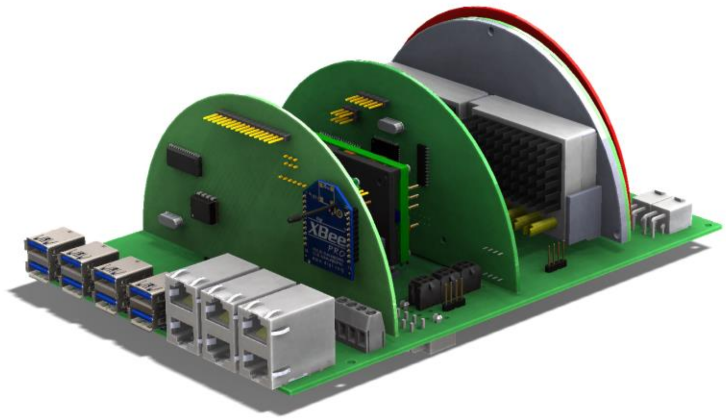

Figure 7. Electrical backplane with three daughter boards slotted in it

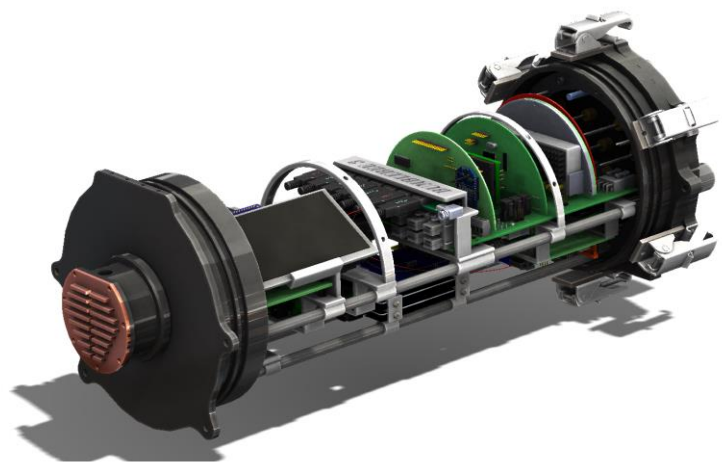

Figure 8. Bumblebee AUV 3.0 electrical rack

AUV backplane is a custom printed circuit board (PCB) with the main functions of:

- Providing power to the peripherals
- Providing data connectivity to peripherals
- Current and voltage monitoring
- Power control

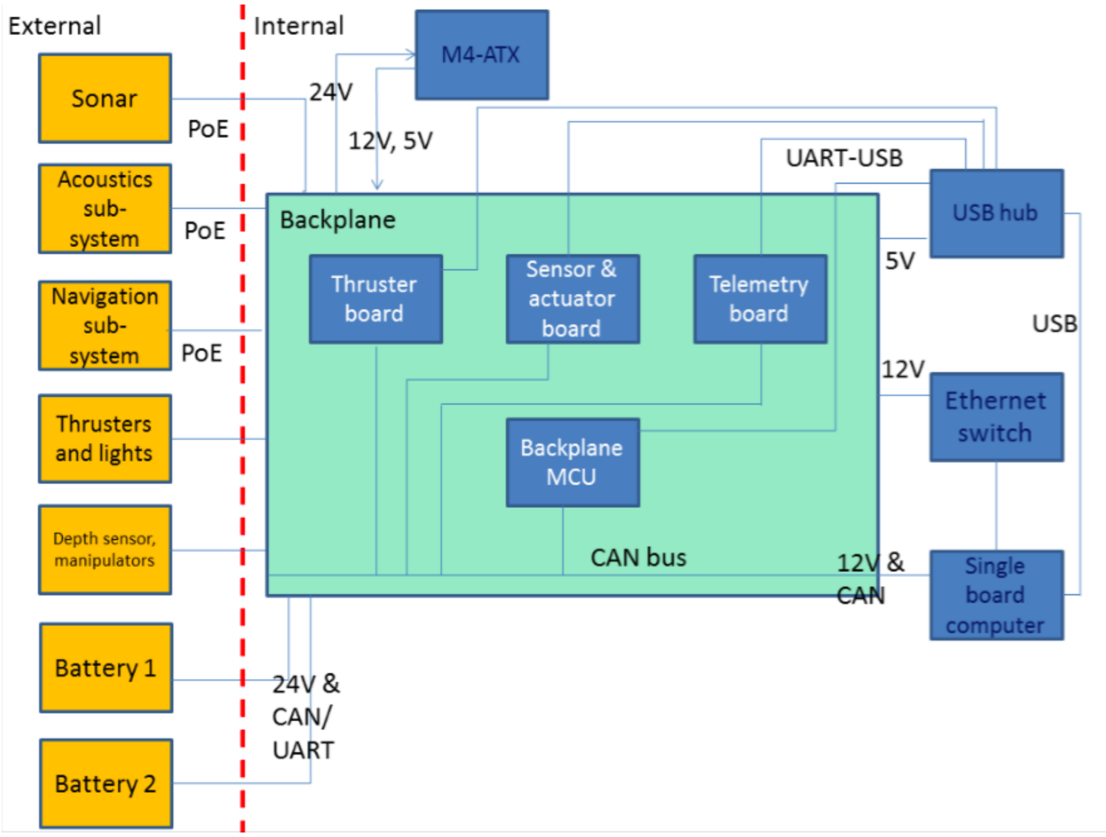

Figure 9. Power and data links between backplane and other major electronics

Figure 9 shows that the backplane is responsible to distribute power to other peripherals. After taking in power from two external batteries, it powers the voltage regulator, M4-ATX with load-balanced 24V output, and the M4-ATX gives back 12V, 5V, and 3.3V back to the backplane. The backplane then routes the different voltages to power respective electronics inside and outside the main hull.

Other than for power distribution unit, the backplane also provides data connectivity from the SBC to other peripherals. There are 6x USB to UART converter circuitries to provide connectivity from the SBC to the Microcontroller

Unit (MCU) of the backplane and the daughter boards. It also has UART to CAN converter, thus allowing the SBC to join in the CAN bus.

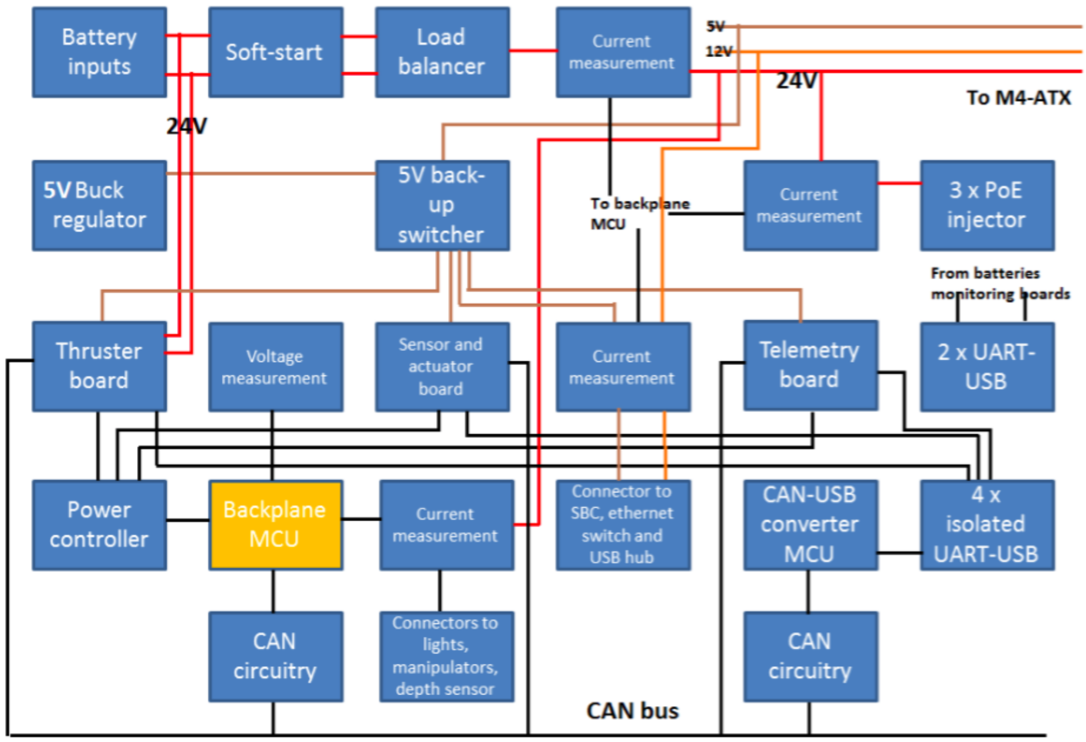

Figure 10. Electrical architecture of the backplane

The power circuitries of the backplane include the soft-start function, load-balancing, and voltage and current measurement.

As the processing unit, the backplane MCU will receive the voltage and current reading and it will control the power input to the three daughter boards: thruster board, sensor & actuator board, and telemetry board. It will also control the power input to the Power over Ethernet (POE) devices through its POE injector feature.

The CAN circuitries consist of CAN controller and transceiver, enabling the backplane to communicate through the CAN bus. It also has a UART to CAN converter. The SBC that communicates with the backplane through UART can now join the CAN bus to talk to other CAN peripherals.

The design of the backplane has been done last year and each feature has been tested individually. However, the bigger challenge is in the integration of the backplane with the rest of the components and making sure that it is reliable during operation.

4 AUV Existing Problems and Solutions

4.1. Problem 1: Unreliable power supply at 5V level

To convert 24V to 12V, 5V, and 3.3V power rails, the voltage regulator used in the AUV is M4-ATX, which is a Power Supply Unit (PSU) from Mini-box. M4-ATX is using buck/boost converter topologies to convert the DC line.

Figure 11. M4-ATX from Mini-box

At times, the 5V line from the M4-ATX would drop below the backplane MCU operating voltage of 4.5V-5V. This voltage drop happened in a short time and it caused the MCU to restart. This was actually the main problem during RoboSub 2015 that prevented the team to achieve the first place. Tests conducted in lab shows that the thrusters are the main cause of this voltage drop.

Figure 12. Changes in the 5V line when thrusters are running

Figure 12 shows the changes in the 5V line when the thrusters are immediately running at full speed. Especially for the brushless VideoRay thrusters, the inductive load causes a voltage drop at a very short time, but long enough to disrupt the power to the MCU. The oscilloscope is using 500mV division, and from Figure 12 it can be seen that the voltage drop is more than 1V.

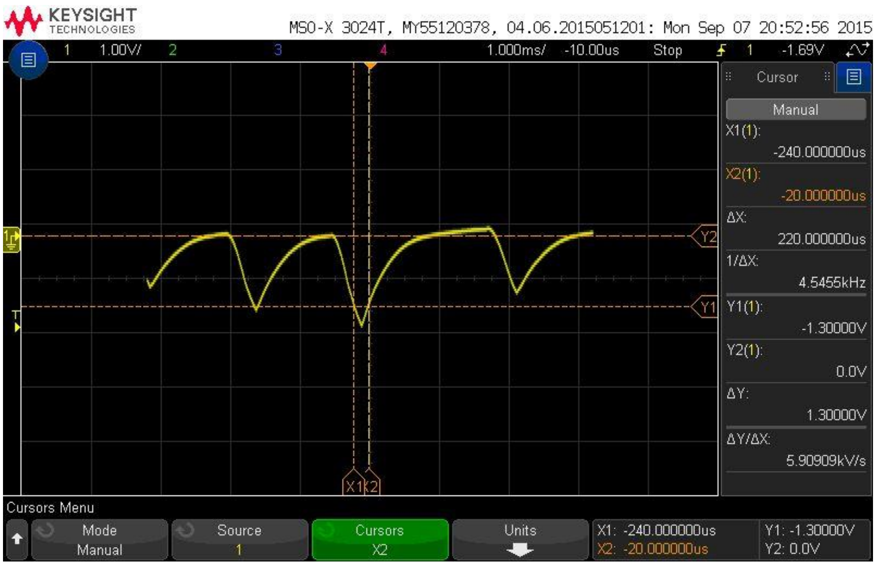

Figure 13. AC coupling to remove DC components

From there, AC coupling capabilities of the oscilloscope is used to eliminate the DC component. A threshold is set such that the oscilloscope will capture the moment of when the voltage is lower than the threshold. From the figure, it can be seen that the power line on the 5V rail experiences a voltage drop of more than -1.3V in the span of 200 microseconds, and this is when the MCU restarted. Sometimes, the voltage drop can be even as low as -1.7V. The testing was done several times to ascertain that the voltage drop caused by the inductive load of the thruster is the main cause of the problem. Out of 10 times the testing is conducted, the embedded system restarted 4 times.

4.2. Solution 1: Different DC-DC converter topology

To understand how to mitigate this problem, a further study on the different DC-DC converter topologies is needed.

DC-DC converter topologies generally divided into two categories: transformer-isolated and non-transformer. In each category, there are several topologies, with some available in both forms. The non-isolated converters are inexpensive solution to many applications and are often used for small voltage conversions. However, unlike the isolated converters, they are not protected against high input voltages or transients (Wurth Electronics, 2012). The isolated converter has more complex circuits and it requires a higher number of components, hence it’s more costly.

According to the datasheet, the M4-ATX uses switching regulator with buck and boost converter topologies. To prevent the transient voltage caused by the thrusters, an isolated converter topology is explored instead. Isolated DC-DC converter provides physical separation between the input and the output through the use of galvanic isolation between the two.

To choose the proper DC-DC converter, it is important to consider the power rating of the whole electronic system of the vehicle.

Components	**Voltage Rating (V)**	**Current Rating (A)**	**Power (W)**
Outside the main hull			
Bandpass filter / pre-amplifier	24	0.5	12
NI sbRIO	24	0.5	12
Imaging sonar	24	0.5	12
GEDC	5	0.5	2.5
AHRS-8	5	0.5	2.5
XSENS IMU	5	0.5	2.5
BeagleBone Black	5	0.5	2.5
Total			**46**
Inside the main hull			
SBC	12	4.25	51
LED Strip	12	1	12
Ethernet switch	12	1	12
Camera & card	12	0.5	6
5x ATMega2560	5	2.5	12.5
Assorted Ics	5	0.5	2.5
Telemetry	3.3	1	3.3
Total			**99.3**

Table 1. Power rating for the electrical components of the vehicle

If an isolated DC-DC converter is going to be used, two isolated DC-DC converters are needed: one for the electronics inside the main hull, and another one for those outside the hull, which are the acoustics sub-system and the navigation sub-system. From Table 1, the isolated DC-DC converter that is to be chosen has to withstand more than 99.3W of power. It is quite challenging to find a 24V isolated DC-DC converter with such rating, and the closest one that is found is a 24V – 24V isolated DC-DC converter by Murata model UVQ-24/4.5-D24PB-C with power rating of 108W. However, for the main hull, since the power rating is too close with the minimum rating calculated in Table 1, this model might not be appropriate. Instead, a 24V – 12V isolated DC-DC converter by Murata model UWQ-12/17-Q48PB-C can be used for testing, since it has higher power rating of 204W.

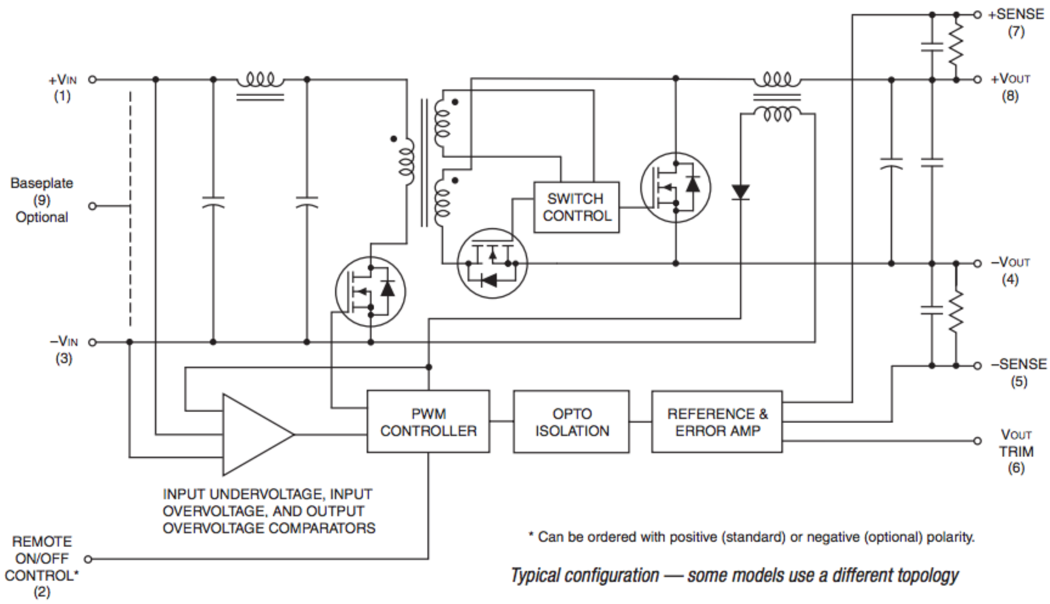

Figure 14. Topology of Murata isolated DC-DC converter (Murata)

From Figure 14, it can be seen how galvanic isolation acts like a transformer, providing physical separation between the input and the output. Isolated DC-DC converters have strong noise and interference blocking capability thus provide the load with a cleaner DC source (Texas Instruments, 2015).

For testing, a 24V – 12V isolated DC-DC converter by Murata model UWQ-12/17-Q48PB-C was tested with the same setup that caused the embedded system of the AUV to die. The DC-DC converter is placed between the battery and the voltage regulator, M4-ATX. After 20 times of running the thrusters in full speed, with the same oscilloscope setup (AC coupling with trigger detection), there was no voltage drop at all. This shows that implementing the isolated DC-DC converter make the system stable and address the power issue.

4.3. Problem 2: Incorrect voltage level in soft-start output

The backplane has a soft-start capability to prevent in-rush current to the system.

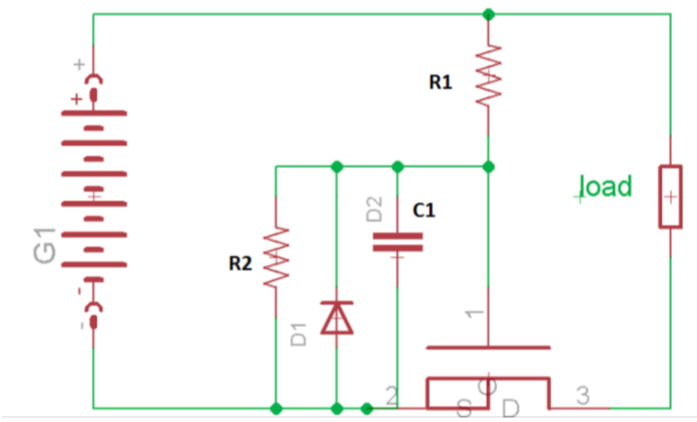

Figure 15. N-channel MOSFET based soft-start circuitry

The circuitry uses N-channel MOSFET that will be turned on slowly by gradually supplying voltage to the V_{GS} gate-to-source voltage. This is achieved by charging the capacitor connected between the gate and the source of the MOSFET. Resistor R1 and C1 act like an RC filter, and the time taken to reach 63% of the steady-state voltage is given by $\tau = R \times C$. The time constant was decided to be 1s, because it was known experimentally that to control the in-rush current effectively, the time constant has to be higher than 10ms. Thus the R1 and C1 were determined to be 1MΩ and 1μF respectively. The value of R2 was chosen to be 1MΩ as well, since the voltage divider network of R1 and R2 should generate voltage that is higher than the clamping voltage of the Zener Diode, which is 10V. By making R1 and R2 to be the same, the voltage at the voltage divider network will be 12V, half the voltage of the supply voltage.

The output of the soft-start circuitry will be routed to the load-balancing feature on the backplane, that will balance the load drawn from the two batteries.

However, the main problem is that, although the steady-state voltage output of the soft-start circuitry should be 24V, in reality it often happens that the output voltage is only around 17V or sometimes even less than that.

4.4. Solution 2: Zener diode as clamping diode

To solve this problem, it is important to understand how zener diode works as a clamping diode to limit the voltage in the circuitry. In the soft-start circuitry, a zener diode is used to clamp the 12V from the voltage divider network down to 10V.

A normal diode usually blocks current that is flowing in reverse direction, and eventually it will suffer damage when the reverse voltage is too high. However, Zener Diode, which is sometimes called “Breakdown Diode”, is purposely designed to break down and clamp the voltage level in the process.

When zener diode is biased in the forward direction, it behaves just like a normal diode passing the rated current, but when reverse voltage that is higher than the rated voltage applied across the diode, Avalanche Breakdown will occur and current will start to flow through to limit this increase in voltage.

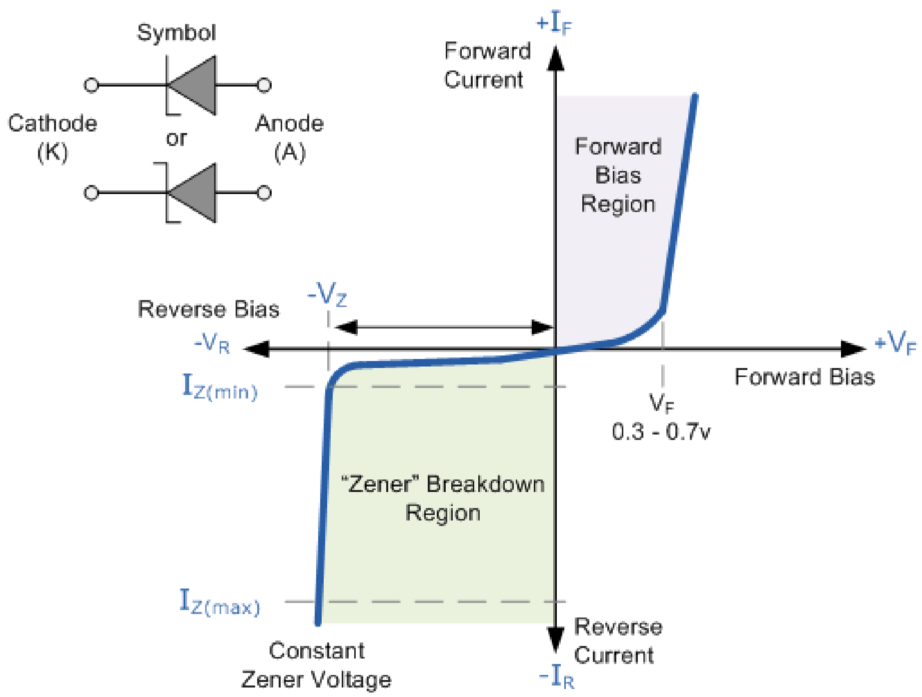

Figure 16. Zener diode I-V characteristic (www.eeweb.com)

The voltage point when the zener diode starts breaking down is denoted as the “zener breakdown voltage”, Vz.

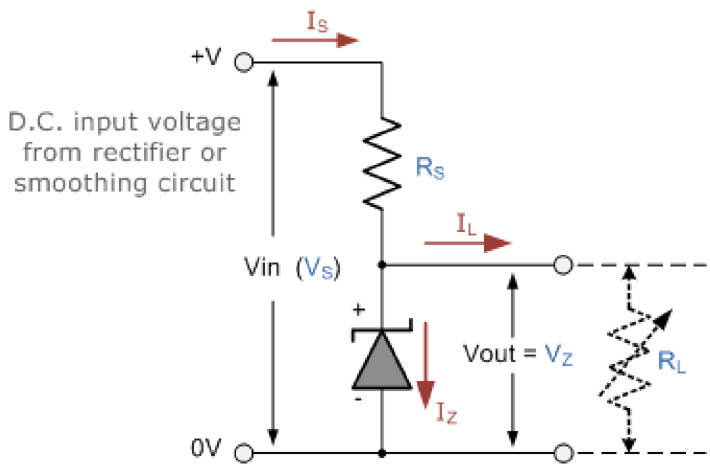

Figure 17. Application circuit for zener diode as a clamping diode (www.eeweb.com)

Figure 17 shows a typical application on how a zener diode is used to clamp the output voltage. The resistor connected in series with the diode limits the current flowing through the circuit. The output voltage is taken across the zener diode. The cathode terminal of the diode is connected to the positive rail, so that it will be operating at its breakdown condition.

The soft-start circuitry in the backplane satisfies the above application circuit of the zener diode. However, the design misses out a small component of the circuit. In the I-V characteristics of the zener diode in Figure 16, it's important to take note that there is a minimum current required for the diode to operate, denoted by $I_{Z(min)}$.

In the soft-start circuitry in Figure 15, the value of R1, R2, and C1 are 1MΩ, 1MΩ, and 1μF respectively. The total effective resistance of R1 and R2 will be 2MΩ, and with supply voltage of 24V, at steady-state voltage, the current flowing to the circuit will be:

$$I = V/R = 24V/2M\Omega = 12\mu A$$

The zener diode used in the backplane is MMSZ4697 from Fairchild Semiconductor. From the data sheet, the test condition at which the zener voltage will clamp to 10V is when the reverse current I_Z is at 50μA.

There is not enough current flowing through the zener diode and hence it was not functioning properly. Thus, a new value set needs to be decided such that more than 50μA of current is flowing through the diode and the time constant of the RC filter in the circuit is more than 10ms. A new set of value for R1, R2, and C1 is to be: 10kΩ, 10kΩ, and 10μF.

$$\tau = R \times C = 10k\Omega \times 10\mu F = 0.1$$

$$I = V/R = 24V/20k\Omega = 1.2mA$$

The time constant is reduced to 0.1s, but it is still significantly higher than the required 10ms. After changing the value of the resistors and capacitors, the output of the soft-start circuitry is giving the correct voltage level of 24V.

4.5. Problem 3: Unreliable USB to UART connection

The backplane features a USB to UART converter that provides communication between the SBC and the MCU in the backplane and the daughter boards. Although the prototype of the circuit works, it is observed that there are a lot of problems with the connection during operation.

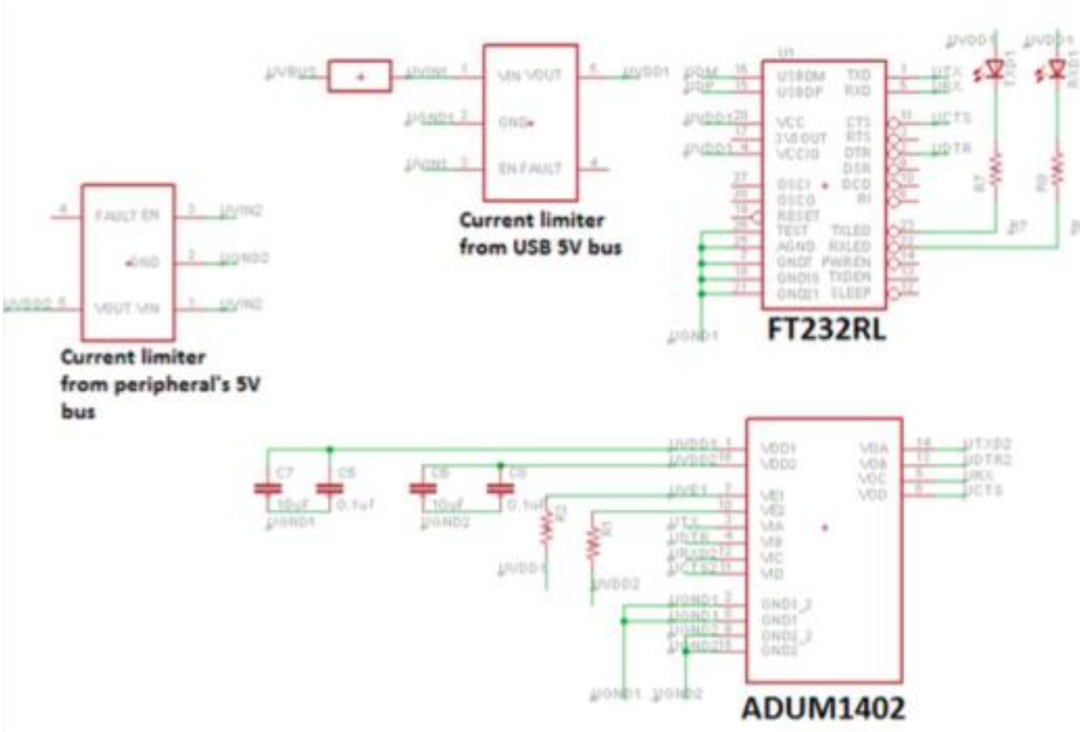

Figure 18. The USB to UART converter circuitry

The USB to UART converter circuitry consists of three main components: the current limiter load switch, the USB to UART converter IC FT232RL, and the opto-isolator IC ADUM1402. The circuitry design was unreliable that many times, the simple act of plugging in the USB cable to the USB connector may kill the USB to UART converter IC, the load switch, or the opto-isolator IC.

4.6. Solution 3: Proper circuit design and Electrostatic Discharge (ESD) protection

At closer inspection, there are many improvements that can be done on the circuit. Some of them are, for example, designing PCB that is suitable for differential signaling and ESD protection, putting an on-board ESD protection, and taking care of the grounding of the USB connectors.

4.6.1. Differential Signaling PCB layout

With the use of FT232R for the USB to UART IC, there are some guidelines that were not implemented in the current backplane design.

In USB connection, data transfers require two signals that are complementary of each other. This is called a differential pair. Differential signaling is also used in other technologies such as Ethernet and RS-485. Especially for USB, there are specific requirements mentioned in the USB 2.0 specifications (Intel, 2000) regarding shielding, signal, and power conductor.

USB connector at the PCB consists of 4 main signals: VBUS (5V power), Ground, Data Plus (DP), and Data Minus (DM). DP and DM are the differential pair. According to USB 2.0 design guidelines, these two signals must be closely matched with the following characteristics:

1. Equal length: Both the DP and the DM signals must have equal trace length. If one is longer than the other, it will affect the timing of the signals and may result in data errors.
2. Impedance: the impedance of the twisted pair cabling in the USB cable must match the impedance in the PCB in order to minimize signal reflections. USB signals are 90Ω differential to each other / 45Ω each to Signal Ground.
3. No stubs: when adding other components, such as Transient Voltage Suppressors, the DP and DM signals should not have any T's to minimize signal reflections.

4. Ground planes: there should not be any splits in the plane directly under DP and DM
5. Overall length: the DP and DM signals should be made as short as possible, with trace length less than 18 inches.

Figure 19 shows several routing violations that should not be done.

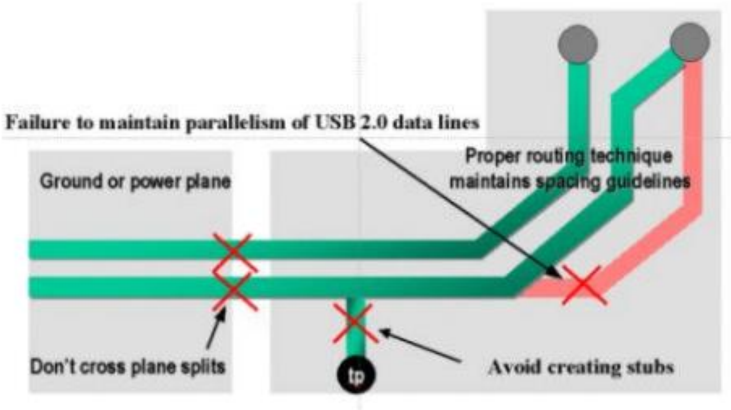

Figure 19. PCB design guide for differential pair (Intel, 2000)

Figure 20 shows some violations to the guidelines, namely: DP and DM in the backplane are crossing planes at the other layer, the gap between DP and DM are not kept the same, and the trace lengths are different.

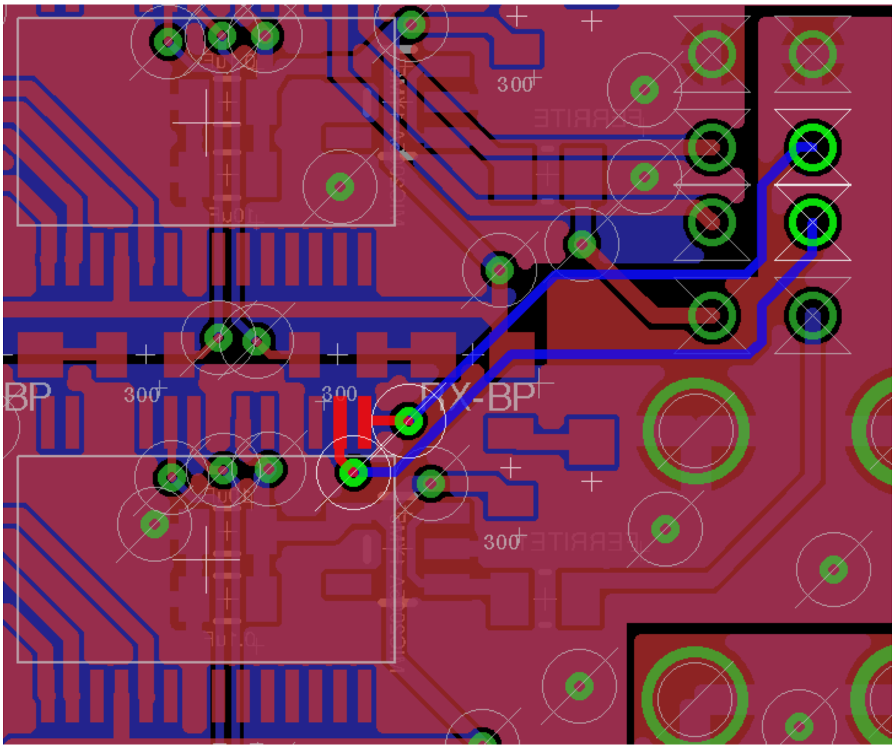

Figure 20. USB differential pair routing in the backplane

The PCB layout of the backplane has to be re-designed to follow the proper guideline for the USB signals.

4.6.2. Electrostatic Discharge (ESD) Protection

The failure for the ICs in the USB to UART converter circuitry might be due to lack of ESD protection circuit in the backplane. ESD protection is important to prevent component or system failure resulting from externally induced high-voltage level impulses. Humans, furniture, and simple materials such as paper or plastic generate ESD pulses. An ESD event from a human can exhibit rise time in the nanoseconds range, with peak impulse currents ranging from a few amperes to greater than 30A (Kularatna, 2000). The backplane doesn't have any casing and human handles it regularly. ESD protection is an important component that should be added.

A robust ESD system design involves factoring in multiple elements such as enclosure, PCB design and layout, ESD ground paths, system wiring and interconnects, etc. The ESD protection designs that will be discussed are the ones that are relevant to the current backplane design.

Following a guide from Texas Instruments (2012), Improvements that are done to the backplane for ESD and EMI protection are:

- Keeping traces as short as possible to reduce trace inductance.
- Keeping sensitive signal traces away from PCB edges.
- For the decoupling capacitors, the one with low effective series resistance (ESR) and effective series inductance (ESL) is used.
- The decoupling capacitor is placed close to the IC power pins
- The trace from the decoupling capaciotrs to the ground is thick and short.

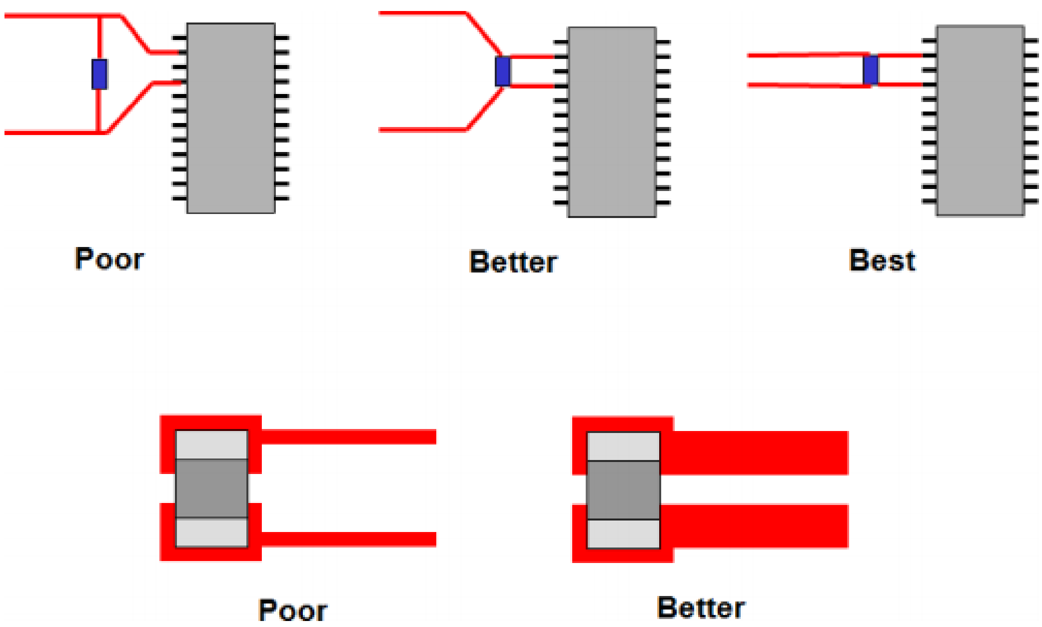

Figure 21. Design guidelines for bypass capacitor (FTDI, 2013)

The manufacturer of FT232RL IC recommends the use of Transient Voltage Suppressor (TVS) as an additional ESD protection on the USB DP, DM, and VBUS signal, as shown in Figure 22. The TVS should be placed next to external connection points, such as USB connectors. This will provide the shortest current path to ground, and hence minimizing the damage elsewhere on the PCB (FTDI, 2013).

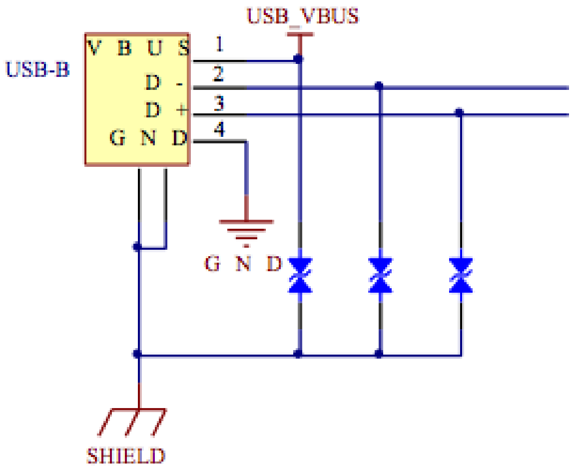

Figure 22. Recommended use of TVS on USB to UART converter circuitry (FTDI, 2013)

This extra ESD protection is also needed to protect the load switch IC in the AUV backplane. MIC2005 is the load switch IC used for over-current protection. However, it is specified to be ESD sensitive and in the case of high current, it will only switch off the output after 700us. On the other hand, ESD happens in the range of nanoseconds.

4.6.3. Ground

As mentioned above, USB connectors have four main signals: power, ground, and two data signals. In addition to that, USB connectors usually provide connection to the shield on the USB cable. In using the USB to UART converter IC FT232RL, the manufacturer, FTDI, noted that it is best to avoid directly connecting the USB shield and the signal ground on the PCB. Instead, a zero ohm resistor can be used for a DC path, or a capacitor for high-frequency path between the shield and the signal ground.

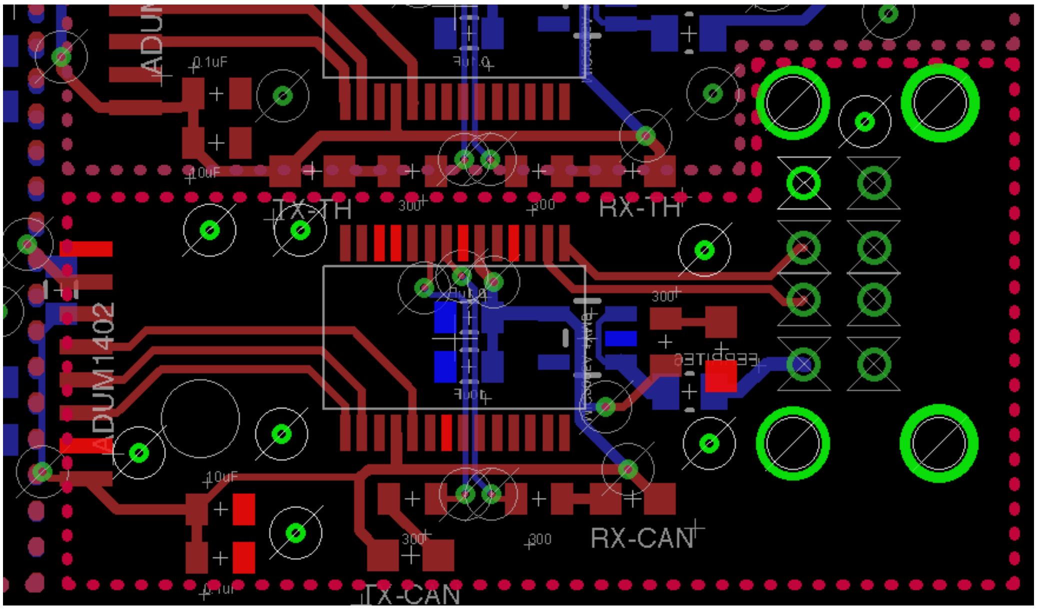

Figure 23. USB ground plane on the backplane

Figure 23 shows the ground connection for the USB connector in the backplane. The shield is directly connected to the USB ground plane. Following the guide from the manufacturer, they should be separated with a zero ohm resistor for DC power path or a capacitor for high-frequency path.

4.7. Result

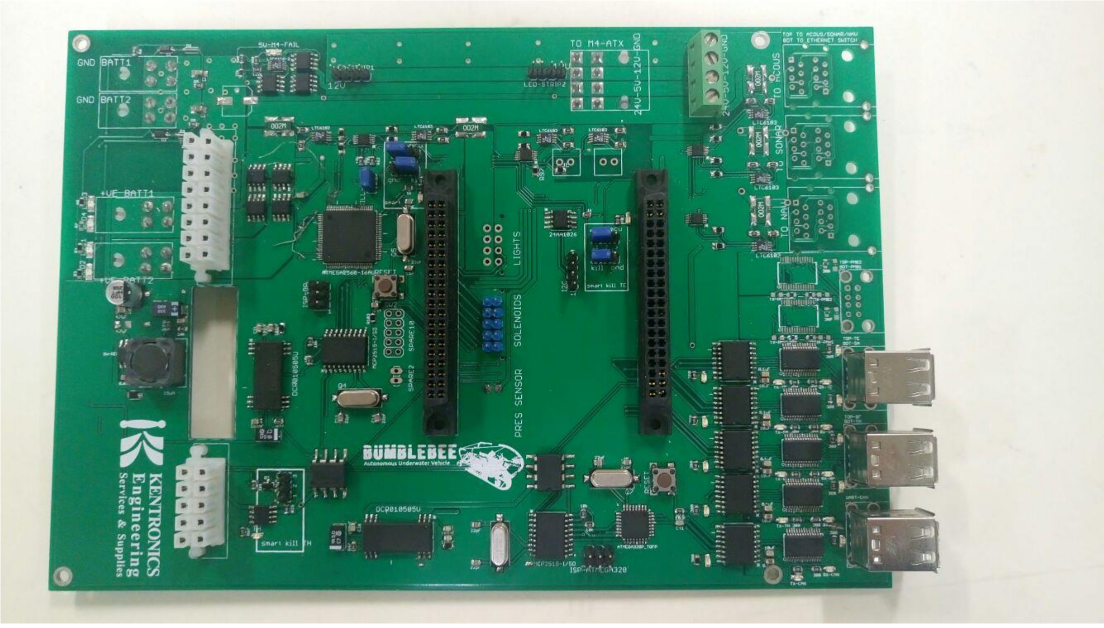

Figure 24. AUV backplane before modification

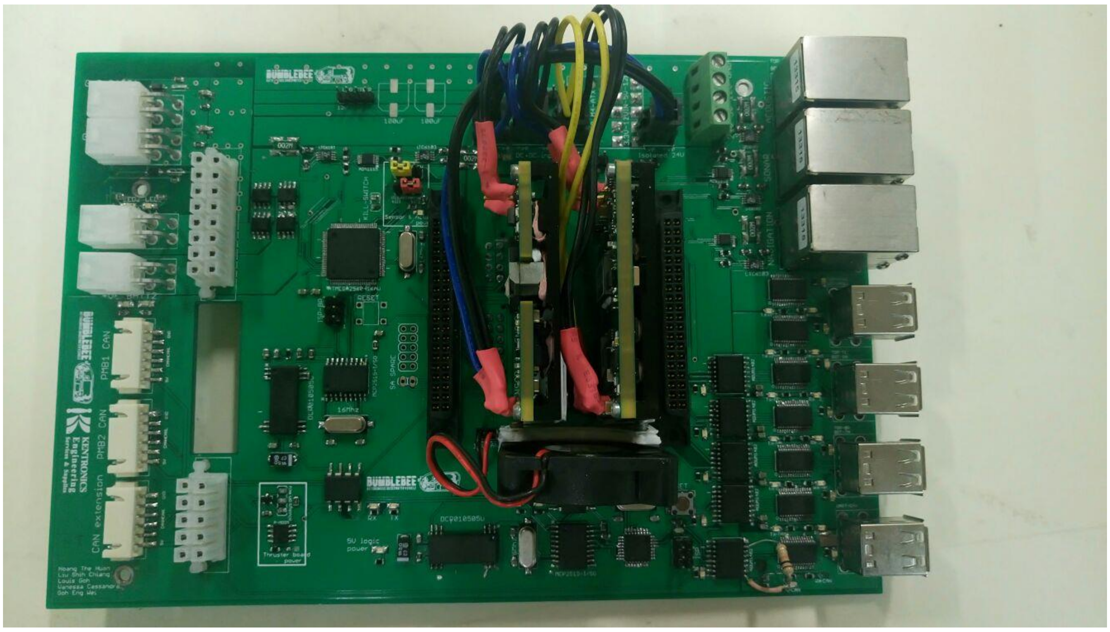

Figure 25. AUV backplane before specification

The modified backplane has been deployed for two months in preparation for Singapore AUV Challenge. So far, there is no other major problem observed.

5 ASV Electronics Components

The lessons learned from the design of the AUV backplane will be implemented on the new autonomous platform that Team Bumblebee is working on: the ASV. A custom board needs to be designed to distribute power and interface the SBC with the thrusters and sensors. Hence, before designing the board, it is important to choose the appropriate components that are suitable for the ASV platform.

5.1. Thrusters

Figure 26. Wave Adaptive Modular Vessel platform (www.wam-v.com)

The Wave Adaptive Modular Vessel (WAM-V) is a watercraft with catamaran-like hull designed by Marine Advanced Research, Inc. Unlike most marine platforms with rigid hulls, the hulls of the WAM-V can move to conform the water surface. As a result, the payload tray at the top is relatively stable when the vessel is moving. Since the payload tray can remain stable during operation, it is suitable for autonomous applications where sensors such as cameras can benefit from the stability. Thus, the 16' WAM-V is selected as the standard platform for the Maritime RobotX Challenge. Table 2 shows the specifications of the WAM-V platform.

Beam	24.3m
Overall hull length	3.94m
Ski length	2.84m
Hull diameter	0.42m
Payload	136kgf (300lbs) max
Full load displacement	248kgf (547lbs)
Draft	0.16m

Table 2. WAM-V specifications (Anderson, 2014)

Taking into account the size and weight of the WAM-V, thrusters with 80lbs of thrust and above are preferable. Two types are considered: Torqeedo Cruise 2.0R or MinnKota Riptide Transom RT80. MinnKota is a well-recognized brand among the boat community, while Torqeedo thrusters have been successfully used by Marine Advance Research Inc., the designer of the WAM-V platform. The Torqeedo Cruise 2.0R has more propulsion power (1120W or 5HP) and have 24-25.9V rated input voltage.

Figure 27. Torqeedo Cruise 2.0R (left) and MinnKota RT80 (right)

	Torqeedo Cruise 2.0R	MinnKota RT80
Max thrust	115lbs	80lbs
Voltage rating	24V	24V
Max current drawn	80A	56A
Control	RS485 with proprietary protocol	Brushed motor controller needed
Cost	SGD$5324	SGD$1650

Table 3. Thrusters specifications

Since the decision on the thrusters involve the Mechanical sub-team, Electrical sub-team, and the Finance sub-team, it is not very easy to choose a model without thinking about it thoroughly. The decision on the thrusters is still under discussion within the team.

5.2. Battery

Since the WAM-V is as big as a motorboat, different types of marine batteries were explored.

5.2.1. Deep-cycle lead-acid boat batteries

Unlike cranking batteries that give short burst of current for a short period of time, deep-cycle batteries are meant for components that sip power at a slower rate for extended periods, such as trolling motors used for boats. A deep-cycle battery can also withstand several hundred charge cycles, while cranking battery is not designed to be totally discharged.

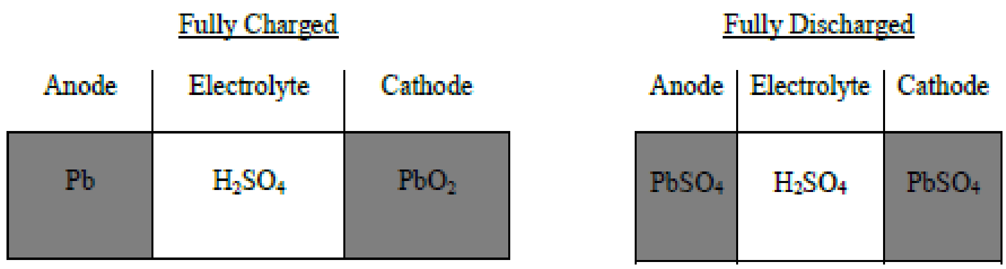

Figure 28. Lead-acid batteries charge state (Albright, Edie & Al-Hallaj, 2012)

Deep-cycle batteries are further categorized into wet cell, gel, and Absorbed Glass Mat (AGM) batteries, depending on the configuration of the electrolyte inside the battery.

The traditional lead-acid battery is referred as wet-cell or "flooded cell" batteries. A properly charged and maintained wet-cell batteries is capable as up to 1,000 recharge cycles. It is also less likely to be damaged by overcharging. A drawback for this type of battery is that it has to be treated with care: the battery compartment must be well ventilated to release hydrogen gas, there is a possibility of spilling the corrosive battery acid, and a regular maintenance needs to be done for the electrolytes. It is also more fragile in an environment with high-vibration, such as boats.

AGM batteries have a dense filling of absorbent glass matting packed tightly between the battery's plates. This results in oxygen being able to recombine with hydrogen gas to replenish the battery's water content, hence unlike the wet-cell battery, there is no need to refill the water. The advantage of AGM batteries is that there is no maintenance needed, except for a periodical external cleaning. Moreover, since the batteries are sealed, the acid inside cannot spill and flammable hydrogen gases aren't released. They are also shock and vibration resistant. The primary disadvantages are its high cost, it is heavier than normal wet-cell batteries, and water cannot be replaced if the battery is accidentally overcharged.

Gel batteries have a liquid electrolyte that is gelled with silicates before the battery is sealed. Similar to AGM batteries, the water in gel batteries does not need to be replaced. They do not require maintenance, they are sealed, and they are also shock and vibration resistant. Another advantage of gel batteries is that they are resistant to over-discharge, which usually may damage other batteries.

However they have a higher initial cost and recharging gel batteries needs charger with special settings dedicated for gel batteries, since they shouldn't be charge with more than 14.1V.

5.2.2. Lithium-ion batteries

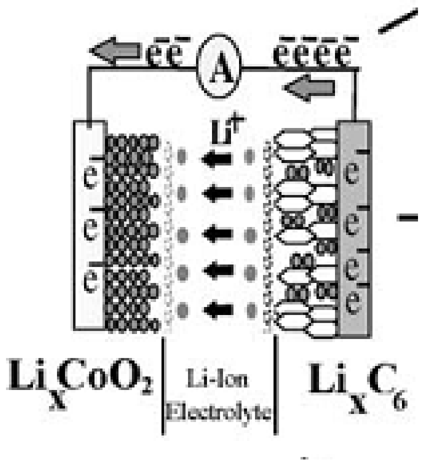

Figure 29. Lithium-ion batteries charge (Albright, Edie & Al-Hallaj, 2012)

The main principle of a lithium-ion battery is that a charged lithium-ion is going back and forth between the cathode and the anode during the charge and discharge.

Usually manufacturers will have variations for the cathode. Different terms like Polymer, Nickel Manganese, Cobalt, etc usually refers to the cathode. Most of the lithium-ion anodes are made of graphite, silicon, or titanium-based materials. Lithium-ion batteries can generally be separated into two groups: Lithium Iron Phosphate (LFP, LiFePO4) and metal oxides (NCM, NCA, Cobalt, Manganese).

All Lithium-ion batteries are "deep cycle", meaning that they have the ability to be fully charged and discharged. To prolong the battery life, each discharge should be limited to 80% of the rated capacity.

5.2.3. Comparison between lead-acid and lithium-ion batteries

Table 4 shows a comparison between lead-acid batteries and lithium-ion batteries, specifically the LiNMC type. However since the chemistries have a wide range of parameter values, the table only shows a simplified comparison of the technology.

	Flooded lead-acid	**AGM and gel lead-acid**	**Lithium-ion (LiNMC)**
Energy Density (Wh/L)	80	100	250
Specific Energy (Wh/kg)	30	40	150
Regular Maintenance	Yes	No	No
Initial Cost ($/kWh)	65	120	600
Cycle Life	1,200 @ 50%	1,000 @ 50% DoD	1,900 @ 80% DoD
Temperature sensitivity	Degrades significantly above 25°C	Degrades significantly above 25°C	Degrades significantly above 45°C
Efficiency	100% @20-hr rate 80% @4-hr rate 60% @1-hr rate	100% @20-hr rate 80% @4-hr rate 60% @1-hr rate	100% @20-hr rate 99% @4-hr rate 92% @1-hr rate

Table 4. Comparison between batteries chemistry (Albright, Edie & Al-Hallaj, 2012)

Lithium-ion batteries have higher cycle life than lead-acid batteries. The cycle life of batteries are affected by depth of discharge (DoD), discharge rate, and temperature. Lead-acid batteries are generally more sensitive to these factors.

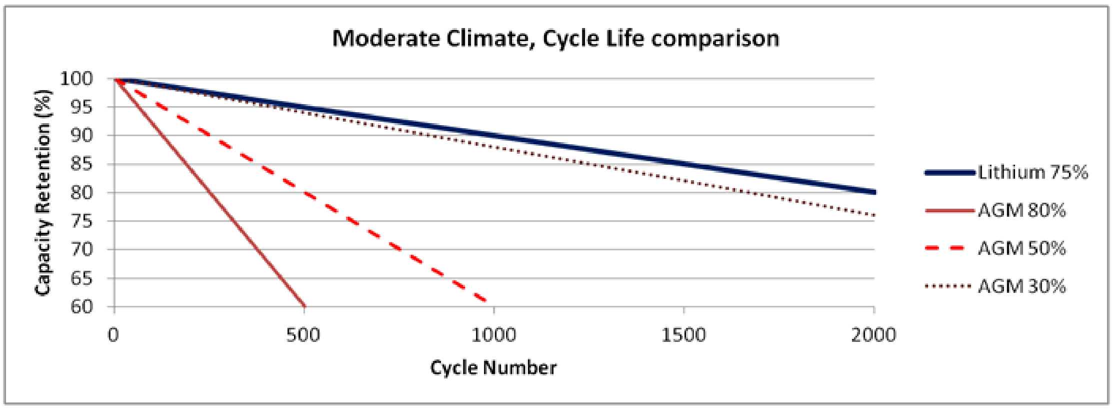

Figure 30. Batteries cycle life in moderate climate (average 25°C) (Albright, Edie & Al-Hallaj, 2012)

Figure 30 shows the cycle-life comparison of the AGM and Lithium-ion batteries. Since cycle-life is highly affected by depth of discharge, the figure above shows the performance under multiple DoD. It can be seen that the DoD of AGM batteries have to be limited at 30% for it to have the same cycle-life time with Lithium-ion batteries. This means that to get comparable lifetime, the AGM battery must have 2.5 times the capacity of the Lithium-ion battery.

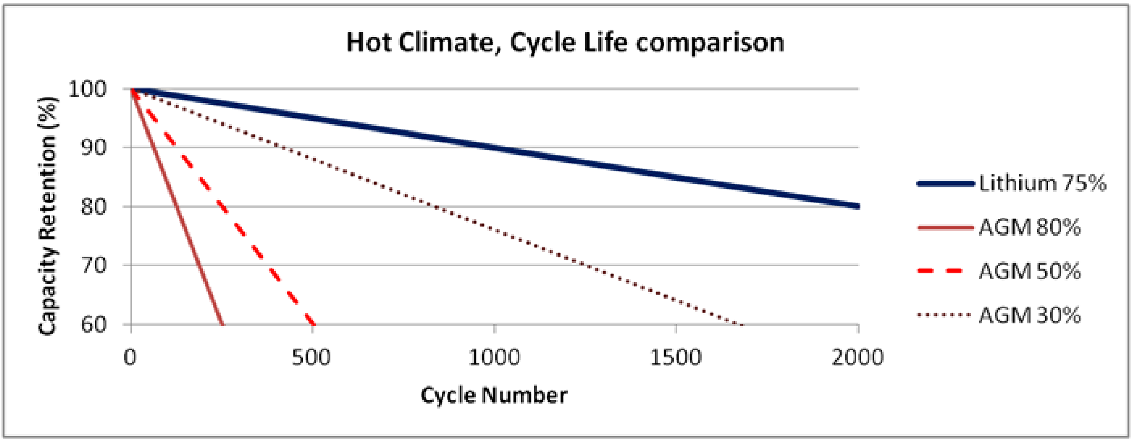

Figure 31. Batteries cycle life in hot climate (average 33°C) (Albright, Edie & Al-Hallaj, 2012)

In hot climates where the average temperature is 33°C, the difference in the performance is larger. The cycle life of lead-acid batteries generally drops to

50% of its moderate climate rating, while the lithium-ion batteries generally remain stable.

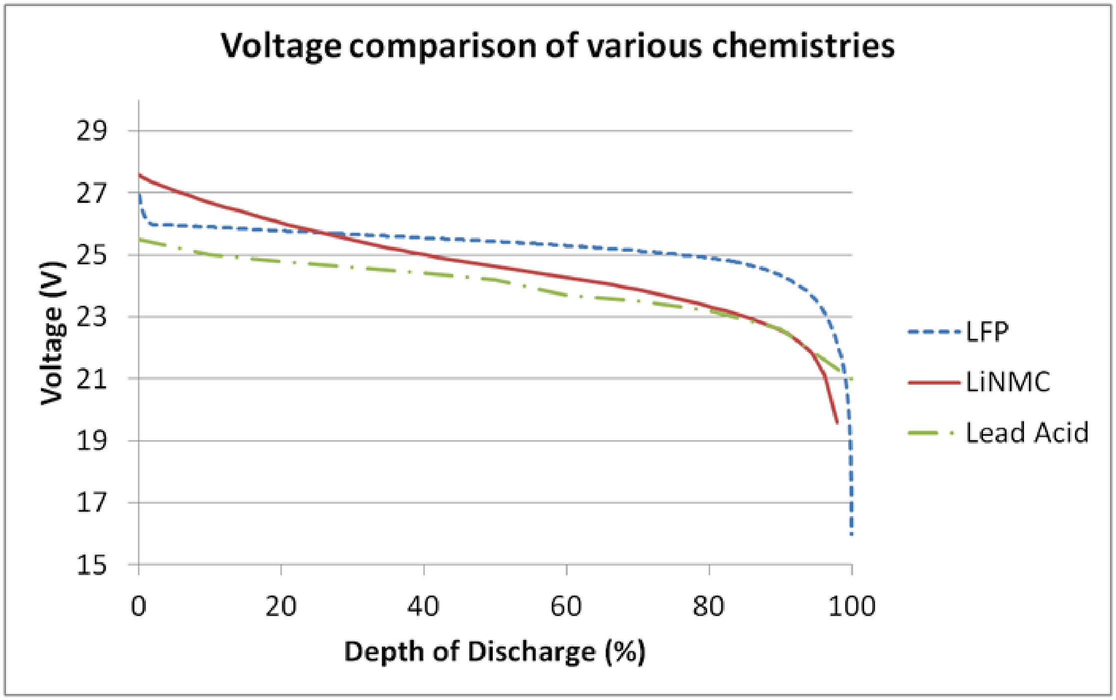

Figure 32. Voltage comparison of batteries (Albright, Edie & Al-Hallaj, 2012)

To evaluate whether lithium-ion and lead-acid batteries are interchangeable, it is important to consider the voltage range of the batteries. The figure above shows the voltage range of batteries that are rated 24V. Although they are rated for 24V, LiNMC is technically 25.9V and LFP is 25.6V. It can be seen that lithium-ion batteries are generally quite similar to the lead-acid battery, but the electronics have to be designed to accommodate the slightly higher voltage level of the lithium-ion batteries.

5.2.4. ASV Battery

Taking into account the factors discussed in the previous section, lithium-ion battery is chosen, mainly because of its energy density and its resistance to hot climate. Heat is one of the main problems of an ASV system, and hence the performance of the battery at high temperature is especially crucial. The battery that is going to be used to power the thrusters from the ASV is Torqeedo Power 26-104 LiNMC battery.

Figure 33. Torqeedo Power 26-104 battery

Capacity	2,685Wh
Voltage	25.9V
Charge	104Ah
Weight	24.3kg
Maximum discharge rate	130A
Communication	RS485

Table 5. Torqeedo Power 26-104 specifications

Learning from the lesson learned in Bumblebee AUV 3.0, the batteries for the thrusters are separated from the battery for the other electronics, so that the physical isolation will prevent the thruster noise affecting the rest of electronics components. The battery used to provide power for the main system of the ASV is the same battery that is used in Bumblebee AUV 3.0.

5.3. Proximity sensors

The proximity sensors will be mounted on the WAM-V and their main function is for object detection during the docking task. There are many technologies that can be used to sense proximity, namely ultrasonic, laser, infrared, and others. However, taking into account the size of the WAM-V and the possible distance between the boat to the object, the proximity sensors need to be able to detect objects of up to 7m distance.

There is not a lot of selection for proximity sensor with such a high range, and hence MB7383 ultrasonic sensor from MaxBotix is chosen.

Figure 34. MaxBotix MB7383 proximity sensor

The MB783 is chosen not only because it has a maximum range of 10m, but also because it is designed to be weather-proof, which is another requirement for all the peripherals on the WAM-V. If the sensor is weather-proof, there is no need for a special casing to be made for the sensor, and thus it will reduce the cost of fabrication of the vehicle.

Resolution	1mm
Read rate	6Hz
Interface	Analog voltage, serial, pulse-width
Operating voltage	2.7-5.5V
Operating temperature	-40°C to +65°C
Maximum range	10m

Table 6. MaxBotix MB7383 specifications

6 ASV Electronics Board

To interface with the electronics peripherals, the ASV will need a custom electronics board with the main functions such as:

- Power distribution
- Data connectivity distribution between the SBC and peripherals
- Sensors and motors interface

As such, some of the features of the ASV electronics board are similar to those of the AUV backplane, but there will be additional ones, such as the interface with batteries and motors.

6.1. Soft start

The soft-start capability is similar with the one described in section 4.2., with the new values for the resistor and capacitor set.

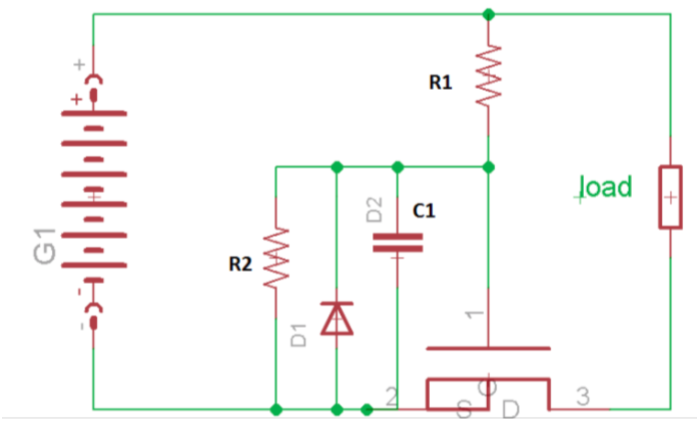

Figure 35. N-channel MOSFET based soft-start circuit

The RC filter from R1 and C1 provides an RC filter that will cause a delay before the gate of the MOSFET is open and power is given to the load. This prevents inrush current from happening.

6.2. Load sharing capability

In the Bumblebee AUV 3.0, to balance the two batteries for the electronics, there is a need to balance the load drawn from each of the battery. As such, a load sharing circuit is implemented using power path switcher IC LTC4416 from Linear Technology. When the difference between the two input sources is more than 100mV, the IC will control a P-MOSFET such that the load will draw current from the battery with the higher voltage.

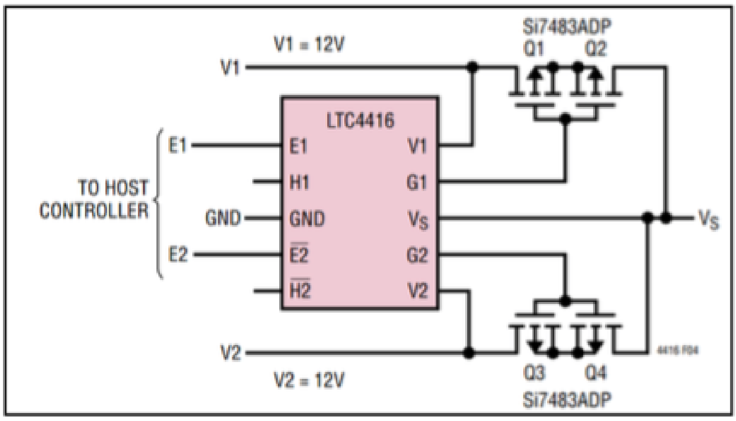

Figure 36. Load-sharing circuit using LTC4416

Similar circuit is implemented on the ASV electronics board to balance the two batteries powering the electrical peripherals in the ASV.

6.3. UART to RS485 converter

The battery for the thrusters, Torqeedo Power 26-104, uses RS485 connection to disclose the battery information. To allow the MCU in the electronics board to monitor the battery status, a UART to RS485 converter circuitry is needed.

For this, RS485 transceiver IC, MAX485 from Maxim Integrated is used.

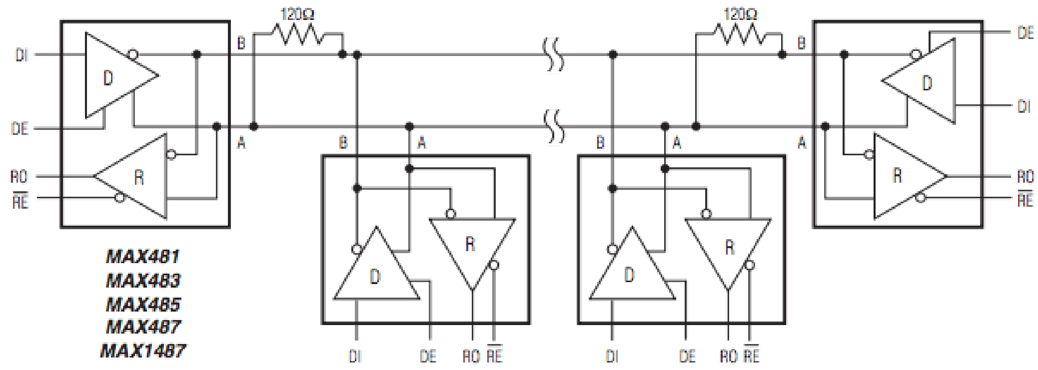

Figure 37. Typical half-duplex RS485 network (Maxim Integration)

Figure 37 shows how four MAX485 ICs can be used to connect UART devices to join in the RS485 network. In the ASV application, there is only one IC needed for the communication with the battery. If Torqeedo Cruise 2.0R thrusters are going to be used, two more MAX485 ICs are needed for the communication to control each of the thrusters.

A breadboard prototype was done with a setup using Arduino to send UART messages through the MAX485 IC, and the RS485 output is connected to a RS485 to USB converter cable from FTDI to be fed into a computer. The computer manages to receive the UART message from Arduino.

6.4. Power over Ethernet (POE) injector

The LIDAR, GigE cameras, and the acoustics sub-system are located outside of the main hull, and they interface with the main processing unit through POE. POE uses RJ45 Ethernet cable to transfer both data and power to the devices. Figure 38 shows the pin allocation for the implementation of POE on the RJ45 cable.

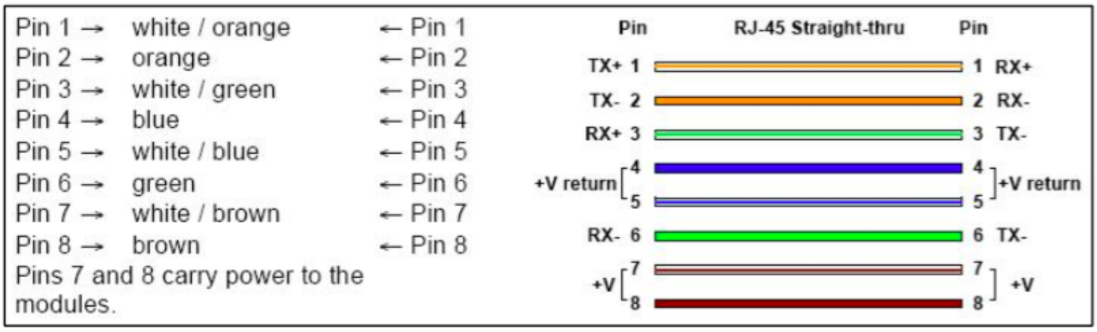

Figure 38. Pin allocation for POE on RJ45 cable (www.wisptech.com)

10Mbps Ethernet only uses two pairs of twisted-pair wire to transmit the data. In other words, out of the four twisted-pair wires inside the RJ45 cable, two of them are not used at all. POE uses those unused pair of wires to transmit Power and Ground, so that power and data can be transmitted using one RJ45 cable.

The POE injector has been working well in the Bumblebee AUV backplane to interface with the imaging sonar and other sub-systems.

Figure 39. Stacked RJ45 connector for POE injector (www.global-sources .com)

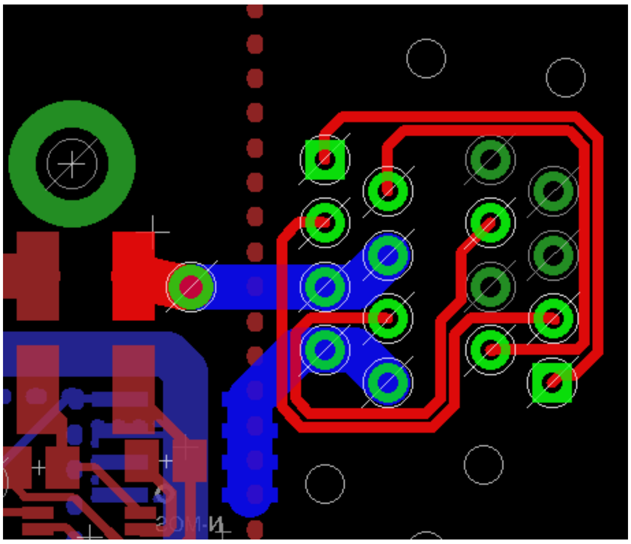

Figure 40. PCB implementation of POE injector

In the PCB implementation, a stacked RJ45 connector is used, and the data signal from one side is routed to the other side. Ground and 24V are also injected into one of the connector that is going to be connected to the POE device.

6.5. Breakout connector

To interface with proximity sensors, there needs to be a breakout for analog input and serial connection from the MCU. Although the mechanism is not decided yet, the ASV will need a manipulator system. For these reasons, the breakout connectors set aside for expansion includes:

1. UART
2. GPIO
3. PWM
4. Power rails: 24V, 12V, 5V, and 3.3V

7 ASV Electronics Boards

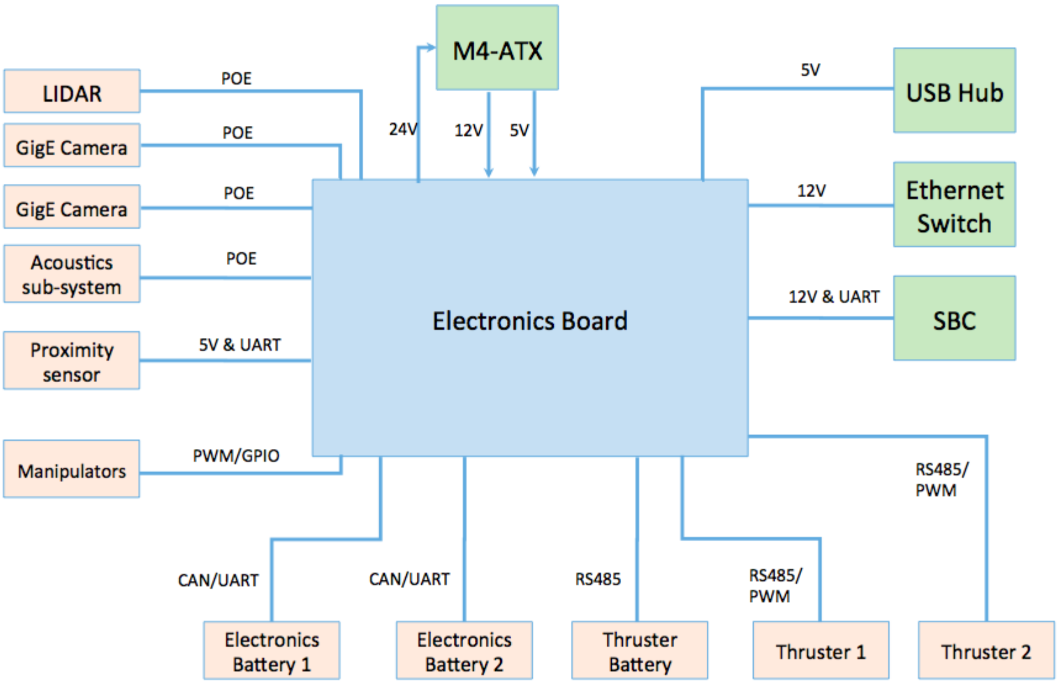

Figure 41. Power and data links between the electronics board and the other ASV components

Figure 41 shows the power and data links between the electronics board and the different peripherals across the vehicle. Inside the same housing as the board, it will provide power for the SBC, Ethernet switch, and the USB hub. Outside the main housing, the board will provide power and data connectivity to the rest of the peripherals in the diagram.

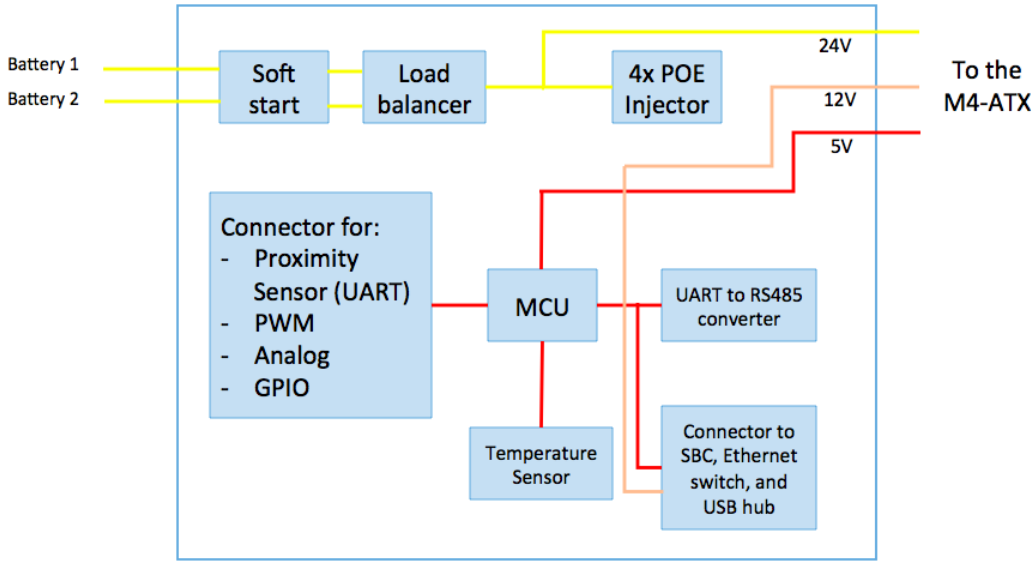

Figure 42. ASV electronics board architecture

Figure 42 shows the architecture of the electronics board. The MCU as main processor of the board will manage the data connectivity to the battery, thrusters, and sensors.

8 ASV Electrical Architecture

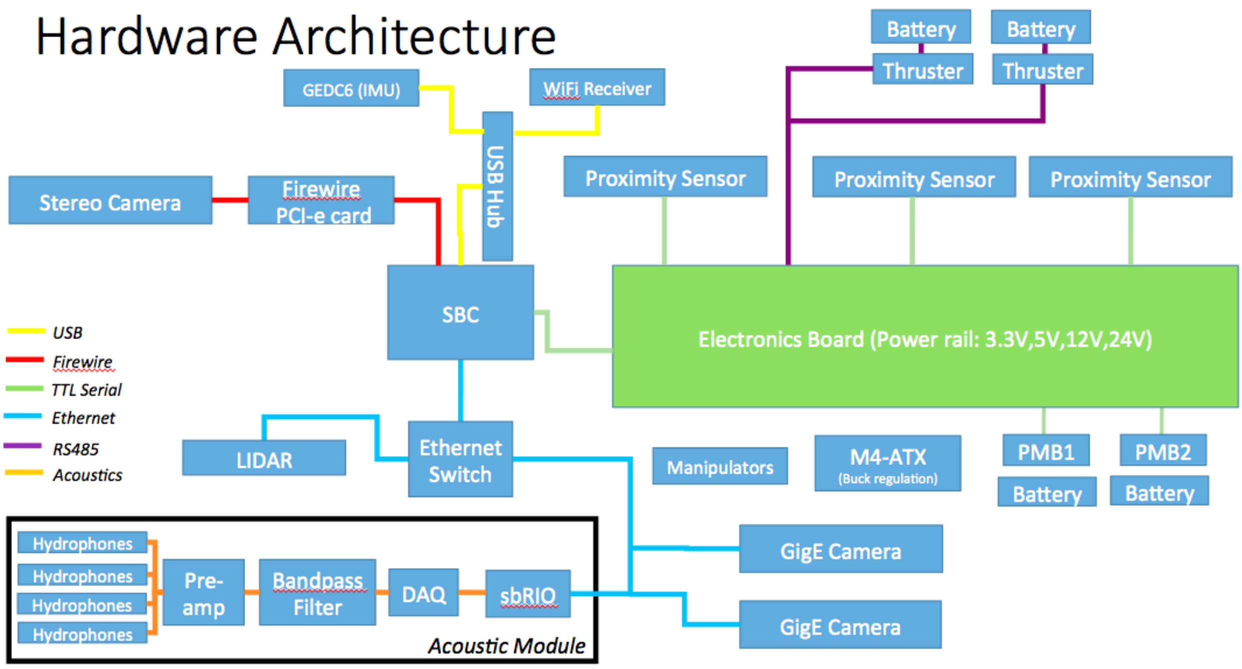

Figure 43. ASV data connectivity architecture

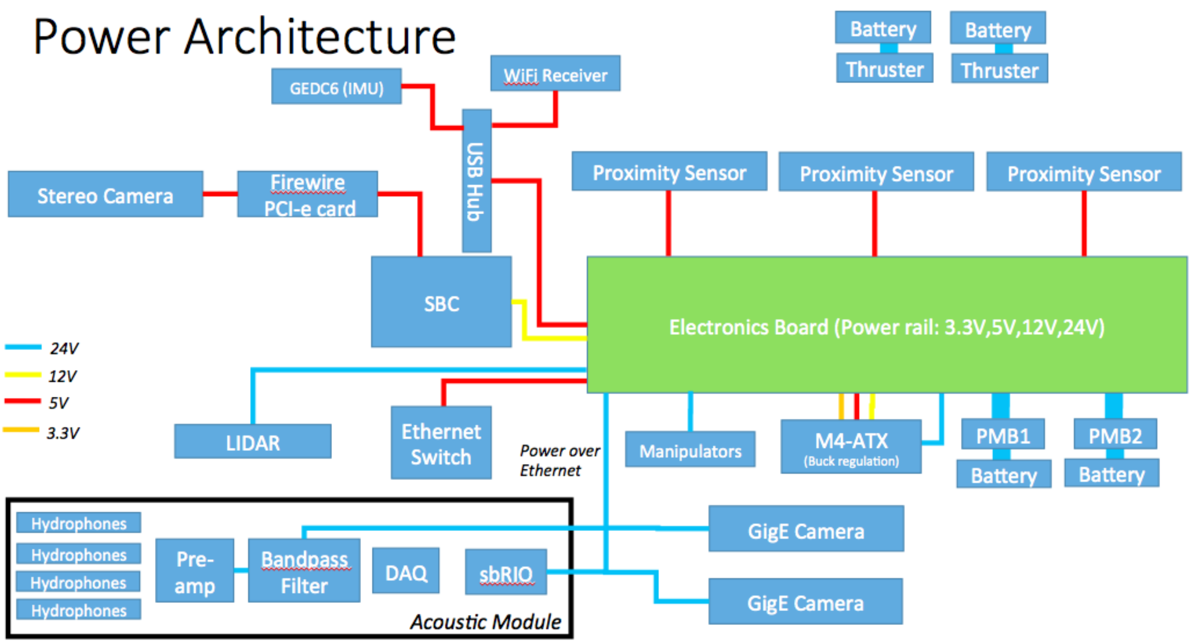

Figure 44. ASV power architecture

The ASV will have two different power sources: the 26V/104Ah battery for the thrusters, and the 24V/7.8Ah battery for the other peripherals, such as the SBC and the sensors. As such, the noise from the thrusters will not affect sensitive electronic components.

For data connectivity, the SBC as the main processing unit interfaces with a LIDAR device, two Gigabit Ethernet (GigE) cameras, and the acoustics sub-system through Ethernet connection. It will also provide FireWire interface for a stereo camera. The communication to the Inertial Measurement Unit (IMU) and the WiFi receiver is through USB connection.

The electrical backplane will receive data through RS485 protocol from the battery and the thrusters (for Torqeedo Cruise 2.0R) or Pulse Width Modulation (PWM) signal (for MinnKota RT80), and through TTL level UART for the proximity sensors and Power Monitoring Board (PMB). These data will then be processed by the MCU on board and passed on to the SBC through UART connection.

9 Conclusion

The implementation of a backplane on an AUV shows the importance of a custom board to distribute power and to manage different communication protocols across the sub-systems. Compared to distributing power using cables, it minimizes the possibility of mechanical failure of cabling.

Unfortunately due to the delay in funding, the expensive ASV peripherals such as the battery and the thrusters are not bought yet, and thus the electronics board designed is not tested with the real devices yet. Undoubtedly there will be problems that will come up during deployment and thus it is important to reiterate the design even after fabrication and testing.

References

Albright, G., Edie, J., & Al-Hallaj, S. (2012). *A Comparison of Lead Acid to Lithium-ion in Stationary Storage Applications.* Retrieved from http://www.altenergymag.com/content.php?post_type=1884

Anderson, M. (2014). *Model-based Control and Control Allocation System for a Wave Adaptive Modular Vessel.* Retrieved from https://wiki.csem.flinders.edu.au/pub/CSEMThesisProjects/ProjectAnde0455/Thesis.pdf

Electronics, W. (2012). *ABC of Power Module.* Wurth Electronics.

FTDI. (2013). *USB Hardware Design Guidelines for FTDI ICs.* Retrieved from http://www.ftdichip.com/Support/Documents/AppNotes/AN_146_USB_Hardware_Design_Guidelines_for_FTDI_ICs.pdf

Intel. (2000). *High Speed USB Platform Design Guidelines.* Retrieved from http://www.usb.org/developers/docs/hs_usb_pdg_r1_0.pdf

Jones, G. (2005). *Miniature solutions for voltage isolation.* Retrieved from http://www.ti.com/lit/an/slyt211/slyt211.pdf

Kularatna, N. (1998). *Power Electronics Design Handbook.* Newnes.

Montrose, M. (2000). *Printed Circuit Board Design Techniques for EMC Compliance.* Wiley-IEEE.

Semtech. (2003). *TVS Diode Application Note.* Retrieved from https://www.semtech.com/images/datasheet/si99-01.pdf

Texas Instruments. (2012, March). *MSP430™ System-Level ESD Considerations.* Retrieved from http://www.ti.com/lit/an/slaa530/slaa530.pdf

Texas Insruments. (2015). *High-Speed Interface Layout Guidelines.* Retrieved from http://www.ti.com/lit/an/spraar7e/spraar7e.pdf

Witherspoon, B. (2008). *Voltage Regulation using Zener Diodes.* Retrieved from http://www.egr.msu.edu/classes/ece480/capstone/fall08/group03/appnotes/files/zener_shunt_regulator.pdf

Wuidart, L. *Topologies for Switched Mode Power Supplies.* ST Electronics.